ELSEVIER

Journal of Nuclear Materials 277 (2000) 315–324

journal of nuclear materials

www.elsevier.nl/locate/jnucmat

Etching of UO_2 in NF_3 RF plasma glow discharge

John M. Veilleux[a,b,*], Mohamed S. El-Genk[a], E.P. Chamberlin[b], C. Munson[b], J. FitzPatrick[b]

[a] *Chemical and Nuclear Engineering Department/Institute for Space and Nuclear Power Studies, University of New Mexico, Albuquerque, NM 87131, USA*

[b] *Los Alamos National Laboratory, Los Alamos, NM 87544, USA*

Received 12 April 1999; accepted 21 June 1999

Abstract

A series of single effect, RF plasma, glow discharge experiments were conducted using NF_3 gas to decontaminate depleted uranium dioxide from stainless-steel substrates. In the experiments, the plasma absorbed power was varied from 25 to 210 W and the pressure from ~10 to 40 Pa. The results demonstrated that UO_2 can be completely removed from stainless-steel substrates after several minutes processing at under 100 W with initial etch rates ranging from 0.2 to 7.4 μm/min. A primary etch mechanism is proposed in which F atoms created in the plasma diffuse to the UO_2 surface and react to form successive intermediates of uranium fluorides and/or oxyfluorides with reactions continuing to form volatile UF_6 which desorbs into the gas phase to be pumped away. Ions created in the plasma are too low in concentration to be the primary etch mechanism, yet they can deliver enough energy to enhance the reaction process. UO_2 etching is a self-limiting process due to the formation of non-volatile uranium oxyfluorides and fluorides which form over the UO_2 surface, slowing or completely blocking the reaction to UF_6.

1. Introduction

The cost of decontamination, treatment, long term storage, and monitoring of transuranic waste in the United States in 1997 in terms of dollars has been estimated at over \$28 000/m^3, compared to \$1800/m^3 for low level radioactive waste [1]. Transuranic waste is defined to be waste containing any alpha emitter with an atomic number greater than 92, a half-life over 20 yr, and an activity of 3700 Bq/g or greater. Objects contaminated with plutonium or americium waste are examples of transuranic waste. Therefore, there is a significant incentive to reduce the quantity of this waste. Possible options include treatment to reclassify transuranic to low level waste, waste volume reduction or better yet a total or partial removal of the transuranic radionuclides from the metal object and full recovery for subsequent recycling or disposal. Unlike mechanical scrubbing and water jet techniques, RF plasma is more effective for removal and recovery of trace radionuclides from surface crevices, can be operated remotely, and provides a better margin of safety for the operator.

Early experiments performed in 1991 by Martz et al. [2] demonstrated that etching of plutonium and plutonium oxide was possible in fluorine-based CF_4/O_2 RF plasma. They measured average PuO_2 etch rates of ~0.03 μm/min at 50 W and 26.7 Pa, and indicated that the rate of Pu metal etching was lower by a factor of 5–10. Some data were acquired for Pu metal etching as a function of pressure in the range from 13 to 80 Pa at 50 W, but were too few and had too much scattering to confidently predict the pressure relationship. The specific surface area of their PuO_2 samples exposed to plasma, varying between 16.9 and 3.48 m^2/g, were not well enough characterized to predict etch rates with confidence. The authors also noted that their gravimetric technique for measurement of mass loss during plasma processing was prone to considerable error.

* Corresponding author. Present address: Los Alamos National laboratory/EWST, MS J514, Los Alamos, NM 87544, USA.

E-mail address: veilleux@lanl.gov (J.M. Veilleux).

0022-3115/00/$ - see front matter
PII: S0022-3115(99)00154-3

Therefore, there was a need to continue this work to better quantify the usefulness and limitations of using RF plasma glow discharge as an effective decontamination technique for transuranic waste.

In an NF_3 RF glow discharge, electrons are created which follow the RF oscillations and collide with neutral particles to cause ionization, dissociation, and other reactions. The most important species for etching are the atomic F radicals created from the dissociation of NF_3 due to electron collisions. The F atoms then diffuse to the surface where they react and volatilize contaminants, such as UO_2. The volatilized contaminants diffuse into the chamber where they are subsequently pumped away, thus cleaning the underlying metal structure. The plasma, a 'quasi-neutral gas', is in a highly non-equilibrium condition with neutral particles near room temperature (~298 K) while the electrons are at significantly elevated temperatures, ~50 000 K. Because the ionization fraction is small, typically <0.001%, the temperature experienced by objects in the plasma is room temperature, and hence heating effects are minimal. As a result, plasma cleaning can be accomplished without destroying the object to be decontaminated.

In this work, a series of single effect RF glow discharge experiments were conducted with NF_3 gas to provide data on the dependence of the uranium dioxide (UO_2) etch rate from stainless-steel surfaces on the absorbed power and pressure. The power and pressure values were varied one at a time and the etch rates of UO_2 from stainless-steel surfaces were measured as a function of immersion time. UO_2 was used to avoid the complex safety and handling requirements associated with experimentation with plutonium, provide data on the decontamination of UO_2 waste, develop procedures on measurement techniques dealing with very small quantities of material, and provide information on the physics of the etching processes. Compared to CF_4/O_2 plasma feed gas [2,3], NF_3 dissociates 10–25 times faster and eliminates the possibility of forming carbon residues in the chamber and on the surface of the sample which would block the etching process. Parallels in the chemistry between UO_2 and PuO_2 can then be applied to the design of future experiments with plutonium oxide contaminants.

Data were collected on the average etch rate of UO_2 as a function of the plasma immersion time, absorbed power, and gas pressure of 17 Pa, the baseline case. Additional experiments were conducted to establish trends at both lower (10.8 Pa) and higher (31–40 Pa) pressures. Comparison of the initial and the remaining radioactivity of UO_2 gave the average quantity etched during a certain immersion time. These results were used to develop a transient, multi-species diffusion model [4] for the etching of UO_2 in the present experiments.

2. Experimental set-up

This section describes the experimental set-up including the plasma system, the method for determining the absorbed power, NF_3 flow rate and plasma pressure, the preparation and specification of the uranium oxide samples, the method developed for achieving reproducible activity measurements of plasma processed samples, and the quantification of the uncertainty in the measurements. The section is concluded with a description of plasma observations during sample processing.

2.1. Plasma system

Experiments were performed using a 13.56 MHz RF plasma system (Fig. 1) with NF_3 gas to decontaminate depleted UO_2 from the surface of stainless-steel substrates. The aluminum test chamber had a volume of 0.125 m^3. An attached fume hood mounted recovery system was used for pumping the gas out of the chamber during experiments. An RF20 power supply provided line power and an adjustable matching network was used to maintain zero reflected power during the experiments. A step-down voltage divider with RF choke was used to measure the effective DC sheath voltage. Details of the chamber and RF antenna are shown in Fig. 2.

2.2. Absorbed power and DC sheath voltage

The power absorbed by the plasma was determined by a subtractive power procedure [5,6] instead of measuring the voltage–current phase angle which would have required extremely precise and difficult measurements. In the procedure used, the peak-to-peak cathode voltage was measured with and without plasma. Without plasma, all power losses were in the matching network and lines. The differences between input power with and without plasma at the same peak-to-peak voltage equaled the power absorbed by the plasma. The fraction of power absorbed to transmitted was ~0.42.

During the experiments, the absorbed power was varied from 25 to 210 W and the resulting DC equivalent sheath voltages ranged from 0.1 to 500 V, respectively. Fig. 3 shows that the measured sheath voltage depends on both the gas pressure and the absorbed plasma power. Increasing the pressure reduced the voltage drop across the sheath.

2.3. Pressure and gas flow

The NF_3 gas flow rate was operated between 3 and 18.5 standard cubic centimeters per minute (SCCM) and the corresponding plasma gas pressures varied between 10.8 and 40 Pa. Pressure was controlled by adjusting the inlet gas flow rate via a rotameter, Omega model

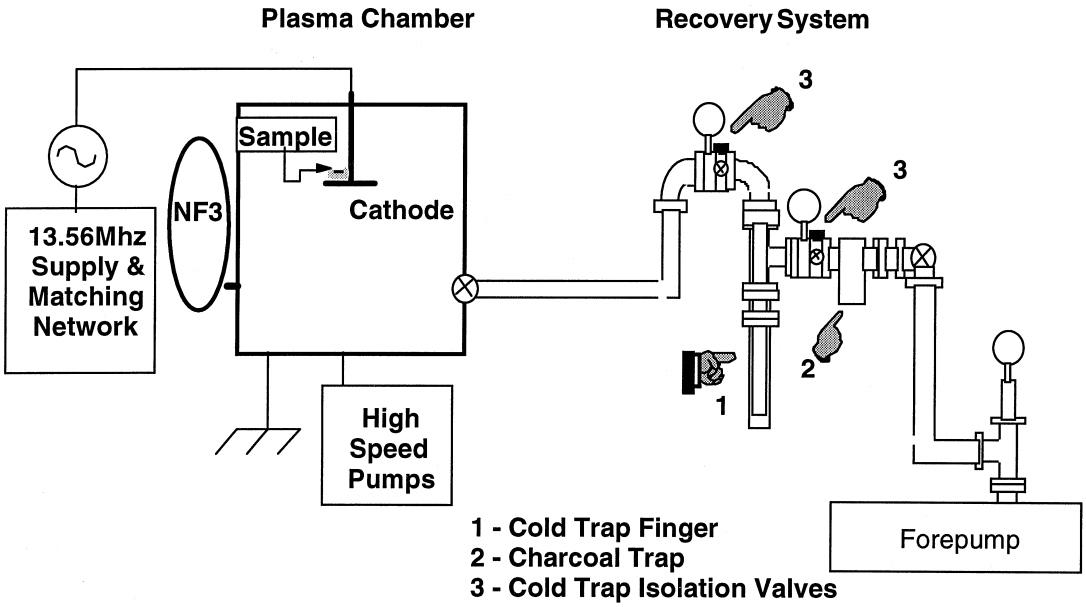

Fig. 1. A line diagram of the RF plasma reactor and recovery system.

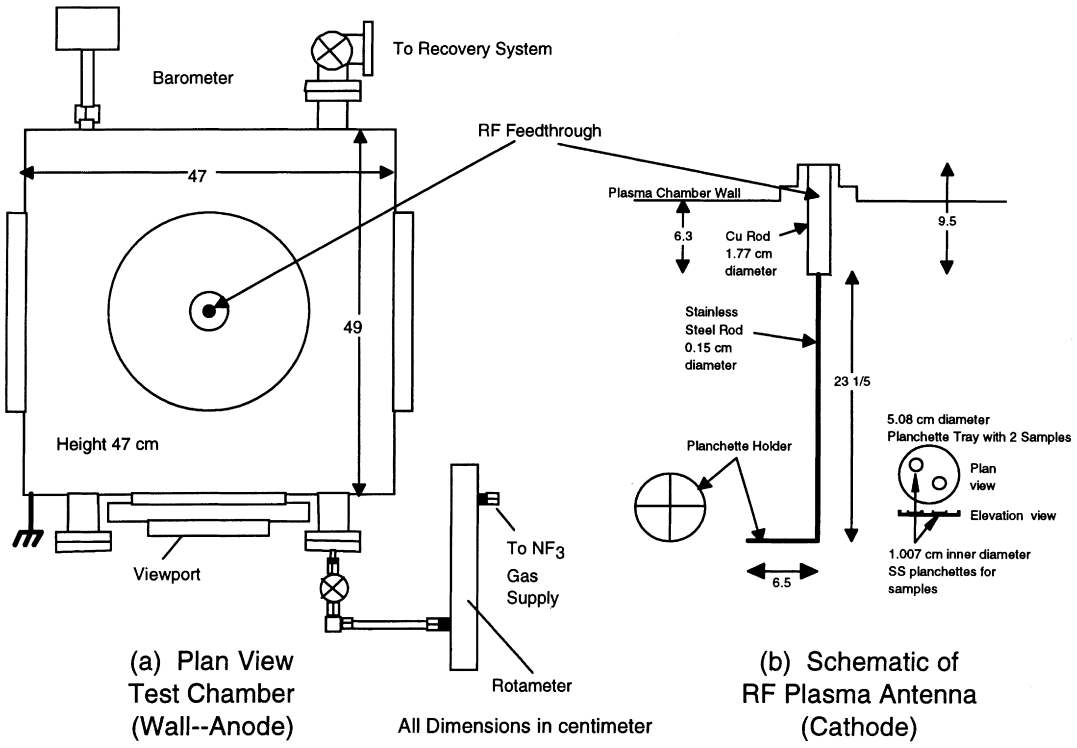

Fig. 2. A cross-section view of the plasma test chamber and a schematic of the RF antenna.

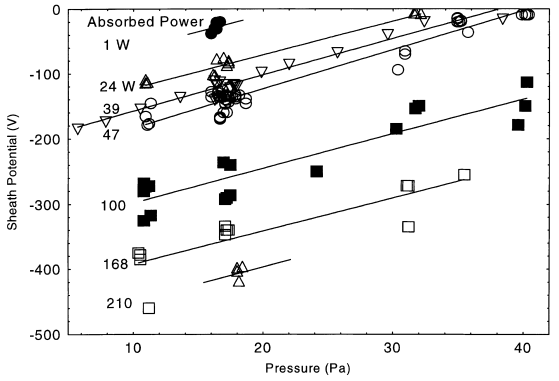

Fig. 3. Measured DC sheath voltage drop in experiments.

SO4-N082-03, and both the pressure and flow rate were kept constant during etching experiments.

2.4. Sample preparation

Depleted UO_2 in test samples was prepared by heating and flaming solutions of uranyl nitrate hexahydrate pipetted in 100 μl increments into cylindrically shaped 1.007 cm diameter stainless-steel planchettes. The resulting amorphous UO_2 had a density of 4800 ± 600 kg/m^3. The measured initial activities for each sample were 129.4 Bq total uranium consisting of 89.5% ^{238}U, 10.2% ^{234}U and 0.3% ^{235}U by activity. Each sample contained 2.36×10^{19} molecules of ^{238}U (99.949% of total U by weight).

2.5. Activity measurements of plasma processed samples

Quantification of the samples' activity following plasma immersion was performed by dissolving the remaining UO_2 in hot 3 M HNO_3, converting the solution to a 0.05 M HNO_3 solution to maintain pH in the range 1.0–1.5 to prevent precipitation, and using the entire solution for maximum detection capability in a Packard UltimaGold™ AB liquid scintillation cocktail. Liquid scintillation counting [7] with alpha/beta discrimination was performed to minimize alpha particle self-shielding and high energy beta particle confounding (215.3 Bq) from ^{234}Th and ^{234}Pa daughters of ^{238}U.

The most probable error in the activity measurement was ±1.9% from over 250 separate samples processed in plasma. This error accounts for uncertainties in: counting statistics, isotope activity ratio, activity of the initial solution, pipette volume, mass measurement, ratio of quantity of radioactive material counted to total quantity, counter efficiency, planchette area, and alpha/beta misidentification.

2.6. Observations

The glow discharge in the chamber during processing had a magenta tinge. The glow was brightest near the antenna at all pressures and filled the entire chamber at 17 Pa at and above 50 W absorbed power. At lower and higher pressures, the glow region shrunk towards the antenna, and was surrounded by a dark region extending from the grounded walls of the chamber to the edge of the glow discharge volume. As power increased, the volume of the glow discharge region expanded outward from the antenna. Fig. 4 depicts the glow discharge region as a function of pressure at 50 W absorbed power.

3. Results and discussion

The experimental results presented in this section correspond to over 250 plasma etching experiments. First, the etching process is described in terms of an example and the parameters used for the analysis are identified. Then, the experimental data on the effects of power and pressure on the initial etch rates are presented. The data suggests that a self-limiting etch effect occurs under certain conditions, and this effect can be understood in terms of the plasma gas species, the radical etchant species, and the surface reactions.

3.1. The etching process

The measured activity of the uranium dioxide removed from the substrate surface normalized to the initial activity of the sample, N_R, is plotted in Fig. 5 versus the plasma immersion time. The data closely follows an exponential function of the form:

$$N_R = N_{R,\max}(1 - e^{-t/\tau}). \quad (1)$$

In the above equation, $N_{R,\max}$ is the asymptotic fraction of UO_2 etched at the end-point, t is the plasma immersion time, and τ is the characteristic etch time. The end-point, as defined in this work, is when all detectable UO_2 in the sample has been etched or the etch rate becomes almost zero, with UO_2 in the sample only partially removed. In the figure, the values of $N_{R,\max}$ and τ, as determined from least squares fit to the data, are 0.96 and 52.7 min, respectively.

The UO_2 etch rate, $J(t)$, can be expressed, based on Eq. (1), as

$$J(t) = \frac{dN_R}{dt} = \left(\frac{N_{R,\max}}{\tau}\right) e^{-t/\tau} = J_0\, e^{-t/\tau}. \quad (2)$$

The term $(N_{R,\max}/\tau)$, or J_0, is the initial etch rate at $t = 0$, and is shown in Fig. 5 as the slope to the curve for N_R

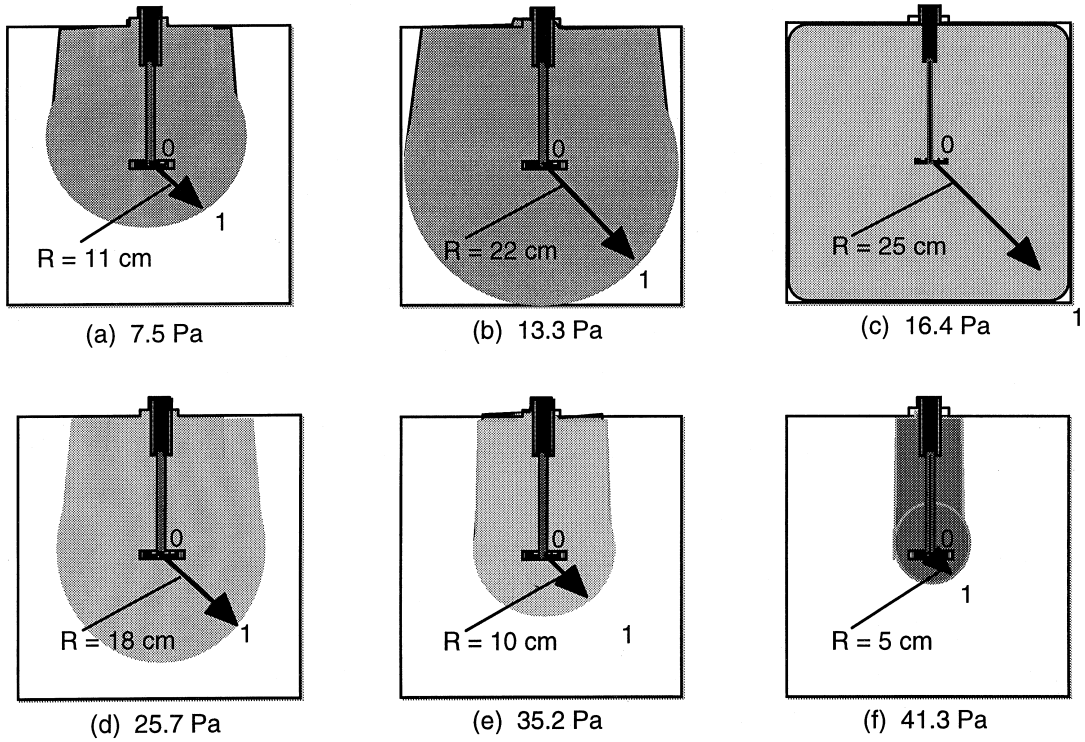

Fig. 4. Glow discharge observations at 50 W absorbed power and different pressures.

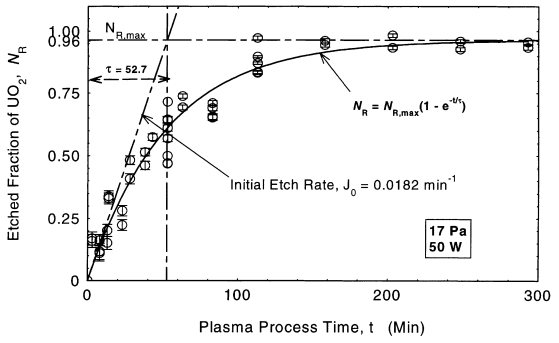

Fig. 5. Fraction of UO_2 etched versus plasma process time at 50 W absorbed power and 17 Pa.

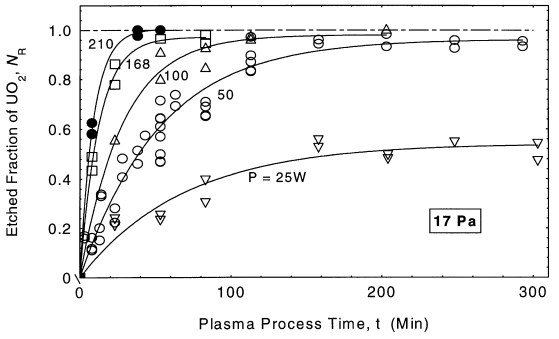

Fig. 6. Effect of absorbed power on the fraction of UO_2 etched at 17 Pa.

versus t (0.0182 min^{-1}). The etch rate $J(t)$ is almost zero after ~4–5 characteristic etch times. The self-limiting nature of the etching process is demonstrated by the term $(1 - e^{-t/\tau})$. This term is a result of the blocking effect of the UO_2 surface during processing to further reaction with the atomic F generated in the bulk plasma to form a volatile UF_6 as explained later in Section 3.5. The blocking term varies from unity at $t = 0$ to zero at the end-point.

3.2. Effect of absorbed power

Fig. 6 shows the UO_2 etch data taken at a constant pressure of 17 Pa, while the absorbed power was varied from 25 to 210 W. The corresponding values of $N_{R,max}$ and τ are summarized in Table 1, along with the initial etch rates, J_0. Except for 25 W, all the UO_2 in the samples was etched to the underlying substrate, given enough time in the plasma. The characteristic etch time

Table 1
UO_2 plasma processing results at 17 Pa

Absorbed power (W)	$N_{R,\max}$	τ (min)	Initial etch rate, J_0	
			(min^{-1})	(μm/min)
25	0.54	68.0	0.0079	0.22
50	0.96	52.7	0.0182	0.50
100	0.98	28.0	0.0350	0.97
168	0.97	12.3	0.0789	2.18
210	1.00	8.9	0.1124	3.11

varied from 52.7 min at 50 W to 8.9 min at 210 W. Three samples (not shown) were processed in plasma for 24 h at 50 W, and there was no detectable [8] UO_2 left in any of the samples. Over 99% of the initial UO_2 was removed at 210 W after 37 min. At 25 W, $N_{R,\max}$ did not reach one, indicating that complete removal of detectable UO_2 could not be achieved at the end-point. The initial etch rate, J_0, in these experiments varied from 0.22 to 3.11 μm/min, depending on the values of the gas pressure and the absorbed power in the plasma. These data show that increasing the absorbed power increased $N_{R,\max}$ and decreased τ, thus increasing J_0, the initial etch rate.

The trend of the results at 10.8 Pa was similar (Fig. 7), except that at both 25 and 50 W, $N_{R,\max}$ did not approach 1.0 before blocking occurred. This shows that even though the sheath voltage increased from −140 V at 17 Pa to −176 V at 10.8 Pa (Fig. 3), the higher energy resulting from ions accelerating through the higher sheath potential was not enough to maintain the etch reactions. The fraction etched decreased as pressure decreased from 17 to 10.8 Pa, implying that the F atom concentration decreased. As power increased above 100 W, however, $N_{R,\max}$ reached 0.96 with τ decreasing to ~30 min.

The highest fractions etched were realized at 32.7 Pa (Fig. 8) with $N_{R,\max}$ approaching one and τ approaching less than 10 min. At 25 W, etch results were similar to the lower pressure results, with blocking occurring before UO_2 could be completely removed. At 180 W, over 99% of the UO_2 was etched away in just 17 min.

At 39.4 Pa (Fig. 9), $N_{R,\max}$ at 50 W was less than unity. These results are similar to the case at 10.8 Pa, suggesting that the combination of pressure and power needs to be optimized to achieve the highest etched fractions. If the pressure is either too high or too low for the power used, the maximum etch fraction decreases.

3.3. Effect of plasma gas pressure

Increasing the NF_3 gas pressure in the experiments increased the fraction etched, N_R, up to a peak pressure, then the fraction etched decreased (Fig. 10). Above 50 W, N_R increased monotonically with pressure in the pressure range examined. In principle, the F atom concentration should decrease with increasing pressure at constant power because fewer NF_3 molecules will dissociate and some F atoms will recombine to F_2 in the plasma and on the chamber walls [9]. However, in our

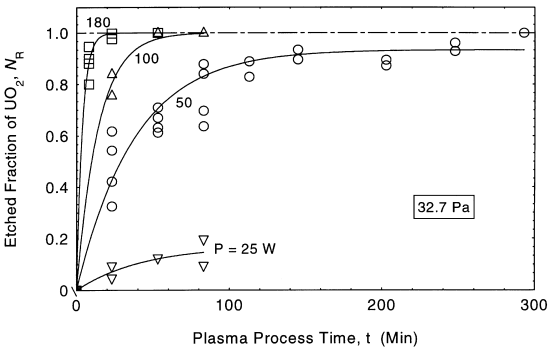

Fig. 8. Effect of absorbed power on UO_2 fraction etched at 32.7 Pa.

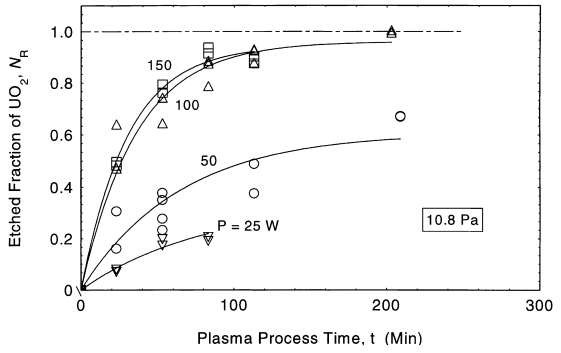

Fig. 7. Effect of absorbed power on UO_2 fraction etched at 10.8 Pa.

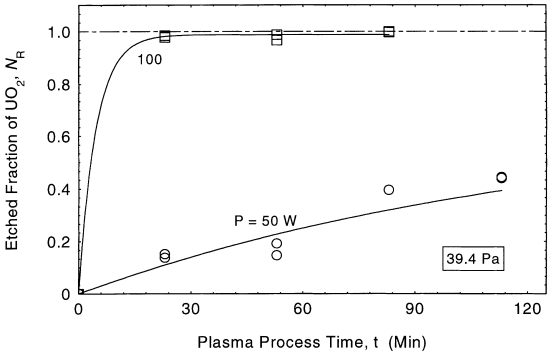

Fig. 9. Effect of absorbed power on UO_2 fraction etched at 39.4 Pa.

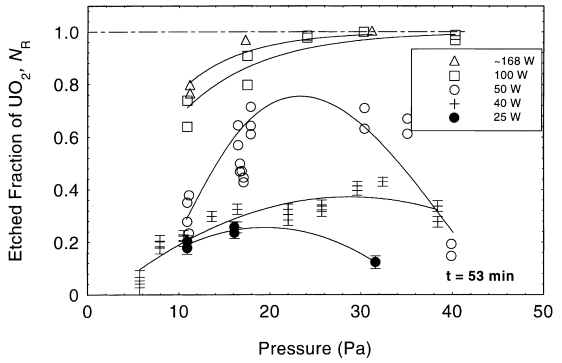

Fig. 10. Effect of pressure and absorbed power on UO_2 etching.

plasma reactor, the brightening of the glow near the antenna and the shrinking glow region implied that the effective plasma volume decreased while ionization increased closer to the antenna. Hence, as pressure increased, the actual F atom density at the sample increased. This effect continued up to a maximum pressure, then the F atom density decreased, as suggested by the decreasing fraction etched as pressure increased further. In the region where etching increased monotonically with pressure, the highest etched fractions were achieved. For example, at 32.7 Pa and 100 W, 99% of the UO_2 in the sample was etched in just 17 min, compared to 37 min at 17 Pa and 210 W.

3.4. UO_2 initial etch rates

Fig. 11 shows the experimental initial etch rates, J_0, at 17 Pa and the trends at other pressures. The baseline data at 17 Pa shows that the initial etch rate increased from 0.2 to 3.1 μm/min as absorbed power increased from 25 to 210 W. Increasing pressure generally increased the etch rate, to a maximum of 7.4 μm/min at 32.7 Pa and 180 W. When power was set too low for a given pressure, the etch rate also dropped as shown by the 39.4 Pa data points, illustrating the effect of non-

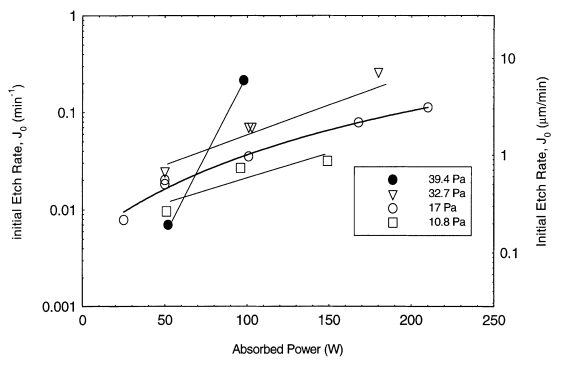

Fig. 11. Initial etching rate of UO_2.

volatile product effects on the etch rate. Decreasing pressure (e.g., to 10.8 Pa) generally resulted in a lower etch rate and this effect was related to the decreasing volume and brightness of the glow discharge near the antenna, and hence lower F atom concentration in the bulk plasma.

The effect of amorphous versus crystalline UO_2 was not studied in these experiments. High temperature reaction experiments [10] suggest that the etch rate with crystalline UO_2 could be lower by a factor of 5.

3.5. The self-limiting etching process

The self-limiting nature of the etching process of UO_2 is explained in this section. The plasma species and hence the likely surface reactions leading to non-volatile products that could block the etchants from adsorbing to the surface and reacting with UO_2 to form a volatile UF_6 are also identified.

3.5.1. The plasma species

To predict the NF_3 plasma species [11–14], a chemical kinetics code, Chemkin [15–17], was validated against other experimental data and then used to quantify the plasma species in this work. The plasma chemistry in this code [18] was modified to include only NF_3 derived species and reactions. The code incorporates 65 ionization, dissociation, attachment, recombination, bimolecular, third body, ion–ion mutual neutralization, charge transfer, and excitation reactions. The validation produced agreement with the measured species in the Si etching experiments [19] of ±5%. A key assumption in this code, which models a continuously stirred tank reactor (CSTR), is a perfectly mixed and uniform plasma throughout the discharge volume. In the current experiments, this assumption was valid only at 17 Pa, where the glow was almost uniform and filled the entire volume for the range of power used. Above and below 17 Pa, the glow region no longer filled the chamber and therefore the model could not be applied, because the effective plasma volume was not constant (Fig. 4).

The plasma species predicted by Chemkin in the experiments at 17 Pa are summarized in Table 2, showing that the primary etchant species are F radical atoms, as further confirmed by other sources [20,21]. The NF_3 is non-reactive, and the other species are too low in concentration to be a factor. The F atom concentration increases with power, and therefore, the etching rate should increase with power, and this is observed experimentally. The ions, while too few in number to contribute significantly to the etching process, can deposit significant energy to the surface, enhancing the reaction processes. For example, the sample substrate temperature rose ~40 K above ambient compared to only 4 K at the walls of the chamber. The high temperature rise of

Table 2
Calculated mole fractions of plasma species at 17 Pa

Species	50 W	100 W
NF_3	0.80	0.61
F	0.15	0.31
N_2	0.03	0.06
F_2	0.01	0.02
NF_2	0.01	0.01
N_2F_4	2.1×10^{-4}	8.3×10^{-5}
N	3.3×10^{-7}	8.2×10^{-7}
N_2F_2	1.6×10^{-9}	7.0×10^{-10}
NF	2.3×10^{-12}	3.0×10^{-12}
N_3	5.2×10^{-57}	7.1×10^{-57}
Electrons	1.7×10^{-9}	6.7×10^{-9}
F^-	6.6×10^{-6}	1.1×10^{-5}
Ions	6.6×10^{-6}	1.1×10^{-5}
Sheath voltage (V)	−142	−261
Ion energy (kJ/mol)	1482	2338

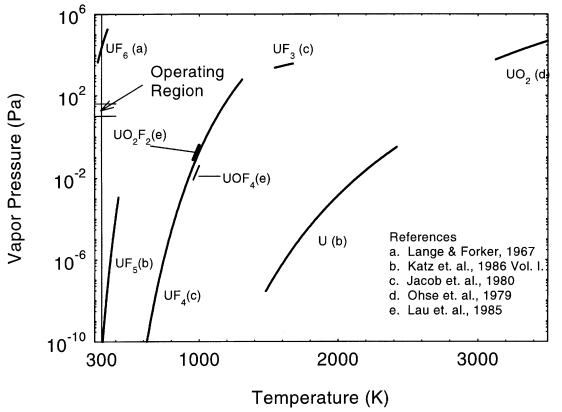

Fig. 12. Equilibrium vapor pressure of UF_x and oxyfluoride compounds.

the sample resulted from exothermic reactions and ion bombardment, whose maximum energy, equivalent to the sheath voltage in electron volts, is reduced by collisions in the sheath [22].

The F atoms created in the plasma diffuse to the UO_2 surface where they are adsorbed and react with UO_2 to produce UF_6. The accumulation of desorbing UF_6 molecules in the sheath slows the flux of F atoms to the surface, reducing the effective F atom diffusion coefficient [4], further blocking or slowing the reaction during the desorption phase. The blocking of the etch reactions that can arise during the reaction steps leading to the formation of UF_6 is described in Section 3.5.2 based on thermodynamic arguments.

3.5.2. Proposed etch mechanism

Since F atoms predominate in the plasma (Table 2), reactions of adsorbed F and UO_2 eventually generate a uranium fluoride gas. Because U forms in the III–VI oxidation states [23], compounds UF_3 through UF_6 and the oxyfluorides of uranium are likely to form. The vapor pressure of UF_6 [24] at 300 K of 24 kPa is well above the operating pressures in the experiments (10.8 to 40 Pa), and therefore UF_6 will desorb into the plasma. The equilibrium vapor pressures of all other compounds [23,25,26], including UO_2 and the oxyfluorides of uranium, are solids at the plasma neutral gas temperature, ~300 K and their vapor pressures are several orders of magnitude lower than the experimental operating pressures (Fig. 12). Therefore, the only product that desorbs is UF_6.

The reaction mechanism to produce UF_6 is complex. The highly reactive atomic F radicals, adsorbed to the UO_2 surface via physisorped van der Waals forces and chemisorption [27], will bind with the valence electrons of the uranium compound molecule to form several non-volatile intermediate compounds of the fluorides and oxyfluorides of uranium as well as UF_6 gas (Table 3).

Table 3
Uranium species and bonding sites for reaction with F radicals

U	O	F	Species	Electronic structure	Maximum bonding sites
1	0	0	U	$[Rn]5f^37s^26d^1$	1
1	0	1	UF	$[Rn]5f^37s^2$	2
1	0	2	UF_2	$[Rn]5f^37s^1$	1
1	0	3	UF_3	$[Rn]5f^3$	2
1	0	4	UF_4	$[Rn]5f^2$	2
1	0	5	UF_5	$[Rn]5f^1$	1
1	0	6	UF_6	[Rn]	0
1	1	0	UO	$[Rn]5f^37s^1$	1
1	1	1	UOF	$[Rn]5f^3$	2
1	1	2	UOF_2	$[Rn]5f^2$	2
1	1	3	UOF_3	$[Rn]5f^1$	1
1	1	4	UOF_4	[Rn]	2
1	2	0	UO_2	$[Rn]5f^2$	2
1	2	1	UO_2F	$[Rn]5f^3$	2
1	2	2	UO_2F_2	[Rn]	2

In Fig. 13, the Gibbs free energy of formation is plotted for each of the uranium species listed in Table 3. This figure provides an indication of which species are likely to form from the starting material, UO_2, shown with a horizontal line. Species above the line require energy while those below the line can spontaneously react. For example, from UO_2 approximately 1000 kJ/mole is needed to form U and release the O_2. The plasma environment provides more than enough energy to form any of these products. The energy is available either from exothermic reactions or from the kinetic energy of ions accelerating through the sheath (Table 2). This energy is sufficient to dissociate UO_2 into U and O_2.

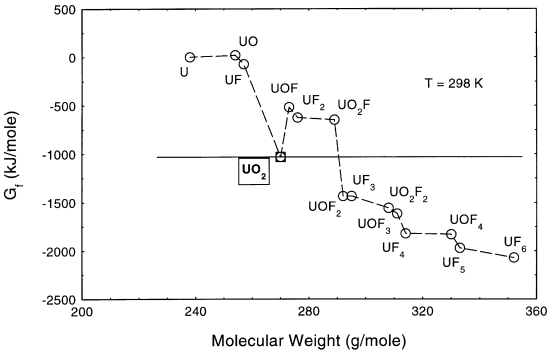

Fig. 13. Gibbs free energy of formation for uranium fluorides and oxyfluorides.

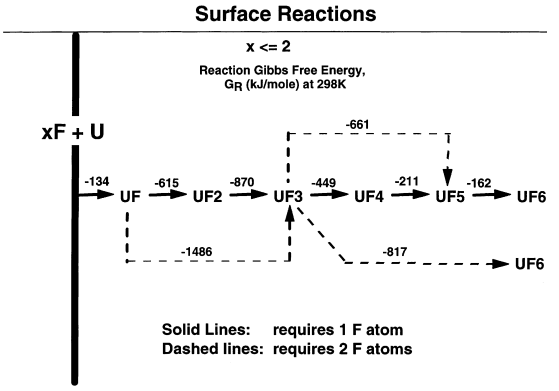

Fig. 15. Gibbs reaction energy, G_R, for U etching.

Consequently, reactions of F with both UO_2 and U as the starting material were analyzed to determine the surface species, based on favorable Gibbs energy of reaction, G_R, and restricting reacting F atom radicals to two or fewer.

The surface products for negative G_R values (or exothermic reactions) from UO_2 starting material is shown in Fig. 14. Reactions involving a single F atom are shown as solid lines while reactions requiring two F atoms are shown as dashed lines. Two products, UO_2F_2 and UO_2F, have G_R values of -650 and -427 kJ/mole, respectively, but because UO_2F requires a single F atom, it has a higher likelihood of forming. From UO_2F, the likely path is to UO_2F_2. From there, two F atoms are required to continue the reaction, but UF_4 is more likely to form than UOF_4 because of its larger negative value of G_R. From UF_4, the most probable sequence is to UF_5 then UF_6. Other reactants requiring two F atoms to proceed are possible, resulting in the formation, for example, of UF_3 and UOF_3, but the reaction products from single F atom reactions are favored. Consequently,

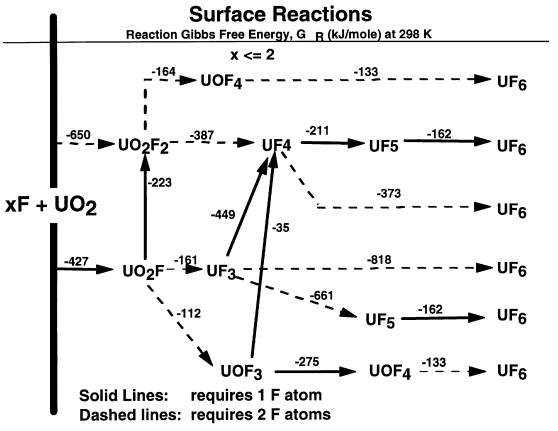

Fig. 14. Gibbs reaction energy, G_R, for UO_2 etching.

the likely reaction products formed from F radicals and UO_2 are uranium fluorides, UF_{3-6}, and uranium oxyfluorides: UO_2F, UO_2F_2, UOF_3, and UOF_4.

Starting with U, the reaction mechanism is shown in Fig. 15. There is a single path to UF from U but because the G_R values of succeeding reactions are significantly more negative, thermodynamics implies that UF will not remain on the surface, but react to form UF_2, then sequentially UF_3, UF_4, UF_5, and UF_6. The reaction from UF to UF_2 or UF_3 is probably very fast, since no stable uranium compounds in the first oxidation state are known [28]. Other paths requiring two F atoms are possible as indicated by the dashed line, but less probable than the first reaction sequence.

Therefore, it may be argued that the non-volatile products likely to form over the UO_2 surface are the uranium fluorides, UF_{2-5}, and the uranium oxyfluorides: UO_2F, UO_2F_2, UOF_3, and UOF_4. These non-volatile products account for the blocking effect previously discussed. If the absorbed power in the plasma power is too low or the feed gas pressure is too high, conditions at the surface may be such that these compounds gradually slow and eventually stop the reaction of F and UO_2. The blocking effect may be reduced by operating with a pressure/power combination that increase the F atom concentration in the bulk plasma and the ion energy to increase the removal of non-volatile deposits. This is supported by the present experimental results (Figs. 6–10).

4. Summary and conclusions

A series of single effect, RF plasma, glow discharge experiments were conducted using NF_3 gas to decontaminate depleted uranium dioxide from stainless-steel substrates. In the experiments, the plasma absorbed power was varied from 25 to 210 W, the pressure from 10.8 to 40 Pa, and the NF_3 flow rate from 3 to 18.5

SCCM. The initial etching rates ranged from 0.2 to 7.4 μm/min. At 100 W and 32.7 Pa plasma gas pressure, over 99% of all detectable UO_2 in the test samples were removed in just 17 min of plasma process time. A primary etching mechanism, based on thermodynamic arguments, is proposed in which F atoms generated in the plasma diffuse to the surface UO_2 and react to form non-volatile uranium oxyfluorides (UO_2F, UOF_4, UO_2F_2) or UF_{2-5} over the UO_2 surface. These products are successively fluorinated with adsorbed F atoms to form volatile UF_6 which subsequently desorbs into the gas phase to be pumped away. Ions created in the plasma are too low in concentration to contribute to the primary etch mechanism, yet can deliver enough energy to enhance the reaction process and contribute to the volatilization of the intermediate reaction products. The self-limiting nature of the UO_2 etching process is believed to be caused by the non-volatile uranium fluorides and/or oxyfluorides intermediates which form over the UO_2 surface, inhibiting or blocking the conversion of UO_2 to the volatile UF_6.

References

[1] R.P. Allen, R.F. Hazelton, Conversion of Transuranic Waste to Low Level Waste by Decontamination – A Technical and Economic Evaluation, Battelle TR PNL-5315, December 1984.

[2] J.C. Martz, D.W. Hess, J.M. Haschke, J.W. Ward, B.F. Flamm, J. Nucl. Mater. 182 (1991) 277.

[3] N.J. Ianno, K. Greenberg, J. Verdeyen, J. Electrochem. Soc. 128 (1981) 2174.

[4] M.S. El-Genk, H. H. Saber, J. M. Veilleux, Analysis and modeling of decontamination experiments of depleted uranium oxide in RF plasma, in: Proceedings of the International Symposium on Heat and Mass Transfer Under Plasma Conditions, Antalya, Turkey, 19–23 April 1999.

[5] C.M. Horwitz, J. Vac. Sci. Technol. A 1 (1983) 1795.

[6] V.A. Godyak, R.B. Piejak, J. Vac. Sci. Technol. A 8 (1990) 3833.

[7] Packard Model 2550 TR/AB Liquid Scintillation Counter with Alpha/Beta Discrimination.

[8] L.A. Currie, Anal. Chem. 40 (1968) 586.

[9] I. Hinz, H. Keller-Rudek, P. Kuhn, H. List, P. Merlet, S. Ruprecht, J. Wagner, Gmelin Handbuch der Anorganischen Chemie: Fluorine, Supplement 2, System-Number 5, Springer, New York, 1980.

[10] T. Yahata, M. Iwasaki, J. Inorg. Nucl. Chem. 26 (1964) 1863.

[11] R.M. Reese, V.H. Dibeler, J. Chem. Phys. 24 (1956) 1175.

[12] M. Konuma, E. Bauser, J. Appl. Phys. 74 (1993) 62.

[13] K.E. Greenberg, J.T. Verdeyen, J. Appl. Phys. 57 (1985) 1596.

[14] T. Honda, W. Brandt, J. Electrochem. Soc. 131 (1984) 2667.

[15] R.J. Kee, F.M. Rupley, E. Meeks, J.A. Miller, Chemkin-III: A Fortran Chemical Kinetics Package for the Analysis of Gas-phase Chemical and Plasma Kinetics, Sandia National Laboratories, SAND96-8216, May 1996.

[16] M.E. Coltrin, R.J. Kee, F.M. Rupley, E. Meeks, Surface Chemkin-III: A Fortran Package for Analyzing Heterogeneous Chemical Kinetics at a Solid-surface-gas-phase Interface, Sandia National Laboratories, SAND96-8217, May 1996.

[17] E. Meeks, J.F. Grcar, R.J. Kee, H.K. Moffat, Aurora: A Fortran Program For Modeling Well Stirred Plasma and Thermal Reactors with Gas and Surface Reactions, Sandia National Laboratories, SAND96-8218, February 1996.

[18] E. Meeks, J.W. Shon, IEEE Trans. Plasma Sci. 23 (1995) 539.

[19] J. Perrin, J. Meot, JM. Siefert, J. Schmitt, Plasma Chem. Plasma Process. 10 (1990) 571.

[20] J. Pelletier, J. Phys. D 20 (1987) 858.

[21] D.L. Flamm, V.M. Donnelly, J.A. Mucha, J. Appl. Phys. 52 (1981) 3633.

[22] M.A. Lieberman, A.J. Lichtenberg, Principles of Plasma Discharges and Materials Processing, Wiley, New York, 1994.

[23] E. Jacob, C. Keller, R. Keim, Gmelin Handbuch der Anorganischen Chemie: Uranium, C8 System Number 55, Springer, New York, 1980.

[24] N.A. Lange, G.M. Forker, Handbook of Chemistry, 10th Ed., McGraw-Hill, NY, 1967.

[25] J.K. Katz, G. Seaborg, L.R. Morss (Ed.), The Chemistry of the Actinide elements, vol. 1, 2nd Ed., Chapman and Hall, NY, 1986.

[26] K.H. Lau, R.D. Brittain, D.L. Hildenbrand, J. Phys. Chem. 89 (1985) 4369.

[27] M.A. Lieberman, A.J. Lichtenberg, Principles of Plasma Discharges and Materials Processing, Wiley, New York, 1994.

[28] S.R. Bierman, E.D. Clayton, R.G. Denning, J. Fuger, H. Gusten, B. Kanellakopulos, K. Rossler, Gmelin Handbook Of Inorganic Chemistry: Uranium, Supl. vol. A6, System Number 55, Springer, New York, 1983.